

In Vivo Three-dimensional Motion Analysis of Chronic Radial Head Dislocations

Junichi Miyake MD, Hisao Moritomo MD, PhD,
Toshiyuki Kataoka MD, Tsuyoshi Murase MD, PhD,
Kazuomi Sugamoto MD, PhD

Received: 15 October 2011 / Accepted: 12 March 2012 / Published online: 13 April 2012
© The Association of Bone and Joint Surgeons® 2012

Abstract

Background Forearm kinematics and interosseous membrane function in chronic radial head dislocations sustained in childhood are unknown. Several procedures have been performed to reduce the radial head on the basis of static preoperative assessment in only one forearm position, but clinical results are not always favorable.

Questions/purposes We investigated the in vivo three-dimensional (3D) kinematics and length changes of interosseous membrane ligaments during forearm rotation in chronic radial head dislocations using 3D CT registration techniques.

Methods We examined 10 patients with chronic radial head dislocations (seven Type 1 and three Type 4

Monteggia lesions). To quantify kinematics, the axis of rotation (AOR) and radial head motion were investigated using computer bone models constructed from CT data placing the forearm in three positions. We also created six interosseous membrane ligaments and calculated their 3D lengths during forearm rotation.

Results In Type 1 lesions, the AOR was located 2.4 mm from the center of the radial head (COR). The COR translated 2.8 mm sagittally and 3.4 mm coronally. Three interosseous membrane ligaments showed little change in length. In Type 4 lesions, the AOR was located 6.2 mm from the COR. The COR translated 10.2 mm sagittally and 4.7 mm coronally. No ligament showed an isometric pattern.

Conclusions In Type 1 lesions, the radial head showed relatively stable motion in the dislocated position and the isometricity of the interosseous membrane remained, which supports the concept of ulnar osteotomy. Conversely, the radial head was unstable and the normal interosseous membrane ligament tautness pattern was disrupted in Type 4 lesions.

Level of Evidence Level IV, diagnostic study. See Guidelines for Authors for a complete description of levels of evidence.

Each author certifies that he or she, or a member of his or her immediate family, has no commercial associations (eg, consultancies, stock ownership, equity interest, patent/licensing arrangements, etc) that might pose a conflict of interest in connection with the submitted article.

All ICMJE Conflict of Interest Forms for authors and *Clinical Orthopaedics and Related Research* editors and board members are on file with the publication and can be viewed on request.

Each author certifies that his or her institution approved the human protocol for this investigation, that all investigations were conducted in conformity with ethical principles for research, and that informed consent for participation in the study was obtained.

This work was performed at Osaka University Graduate School of Medicine, Osaka, Japan.

J. Miyake (✉), H. Moritomo, T. Kataoka, T. Murase
Department of Orthopaedic Surgery, Osaka University
Graduate School of Medicine, 2-2 Yamadaoka, Suita,
Osaka 565-0871, Japan
e-mail: miyake-osk@umin.ac.jp

K. Sugamoto
Department of Orthopaedic Biomaterial Science, Osaka
University Graduate School of Medicine, Suita, Osaka, Japan

Introduction

Radial head dislocation in children may cause osteoarthritis, posterior interosseous nerve palsy, and cubitus valgus deformities in the long term [4, 7, 9, 17, 18]. However, treatment for chronic radial head dislocation is still controversial. To achieve open reduction of the radial head, ligament reconstruction [9, 18, 29, 32], ulnar osteotomy [6, 10], and a combination of both techniques [4, 5, 7, 24, 31, 34, 37] have been proposed. However, the radial

head sometimes remains subluxated or redislocated, even after these procedures [4, 6, 7, 18, 24, 29, 31, 37]. Non-surgical treatment leaving the radial head dislocated also has been advocated [11, 12].

The kinematics of the normal forearm have been investigated using various methods, *in vitro* and *in vivo*. Normally, the radial head in the proximal radioulnar joint is stable during forearm rotation, and the axis of rotation (AOR) passes through the center of the radial head (COR) [3, 14, 20]. Recent *in vivo* and three-dimensional (3D) studies revealed the radial head translated minimally (approximately 2 mm) only in the sagittal direction [3, 14], and the distance from the COR to the mean AOR (d-R) was minimal (approximately 4 mm) [36]. These analytic techniques are advantageous in terms of noninvasiveness, and they can be used in patients with forearm abnormalities [26]. However, *in vivo* 3D kinematics of chronic radial head dislocations have not been reported to date. If the radial head is unstable during forearm rotation, although several procedures have been performed on the basis of static preoperative assessment in only one forearm position, dynamic assessment including several forearm positions may be necessary.

The functional anatomy of the interosseous membrane of the normal forearm also has been investigated by many researchers. The interosseous membrane is a complex of ligaments and membranes, each of which plays a different functional role [8, 22, 25, 33]. Moritomo et al. [22] investigated *in vivo* and 3D change in length of the interosseous membrane ligaments using a novel technique combined with normal anatomic data. They found the central band comprising the broadest and thickest fibers in the interosseous membrane [8, 33], accessory band, and distal oblique bundle are almost isometric during forearm rotation, although there is slight laxity during pronation. The proximal oblique cord and dorsal oblique accessory cord act as check lines, which are taut in pronation. In chronic radial head dislocations without a functional annular ligament acting as stabilizer of the forearm bones, the role of the interosseous membrane is considered crucial. However, in chronic radial head dislocations, the function of the interosseous membrane during forearm rotation *in vivo* is still unknown. In addition, ulnar osteotomy has been performed on the basis of the distal ulna and radius moving together through the interosseous membrane [6, 7, 24, 34].

We therefore investigated (1) the *in vivo* 3D kinematics of the forearm to discover whether the radial head is stable or unstable during forearm rotation, even in the dislocated position, and (2) the *in vivo* 3D change in length of the interosseous membrane ligaments during forearm rotation in chronic radial head dislocation using an advanced non-invasive technique.

Patients and Methods

We studied 10 consecutive patients with traumatic chronic radial head dislocation examined at our institution between 2005 and 2009 (Table 1). The inclusion criterion for this study was radial head dislocation greater than 6 months from the time of initial trauma. Patients with congenital radial head dislocation were not included in this study. There were seven males and three females with a mean age of 16.2 years (range, 8–38 years) included in the study. The mean interval between injury and examination was 109 months (range, 6–372 months). Seven had a Type 1 Monteggia lesion with fracture of the ulna and anterior angulation and anterior dislocation of the radial head, and three had a Type 4 Monteggia lesion with fracture of the ulna and radius and anterior dislocation of the radial head, according to the Bado classification [2]. Eight patients were treated with closed reduction and cast immobilization and two received percutaneous pinning with Kirschner wires. None of the patients had a history of trauma in the contralateral forearm. Informed consent for participation in this study was obtained from all patients or their guardians as appropriate.

Both forearms, from elbow to wrist, were scanned using CT using a low-dose technique (scan time, 0.5 seconds; slice thickness, 0.625 mm; 10 mA, 120 kV) [27] with a LightSpeedTM Ultra 16 CT scanner (General Electric, Waukesha, WI, USA) in three positions: maximum supination, neutral, and maximum pronation. Imaging was done with the patient in the prone position with the arms elevated above the head. Data were saved in DICOM format and sent to a computer. We created 3D computer bone models of the radius, ulna, and humerus from CT data using an original computer program based on the Visualization Toolkit (Kitware, Clifton Park, NY, USA). Volume-based registration [13, 21, 22, 26] was performed semiautomatically to determine relative positions between volume images represented at different coordinates. We expressed transformation of the radius with respect to the ulna in helical axis parameters, which are defined as rotation about and translation along a unique axis [15, 16]. Using this technique, the AOR was calculated [22, 26]. To quantify displacement of the AOR, d-R was investigated according to the method described by Oka et al. [26]. d-R was measured on the axial plane of the proximal radioulnar joint (Plane P) with the forearm in the neutral position (Fig. 1). The distance of COR translation during forearm rotation also was investigated on Plane P. The distance along the line passing through the posterior border of the ulna and the tip of the coronoid process [28] and the distance along the perpendicular to that line were calculated as the distance of sagittal translation of the COR (d-S) and the distance of coronal translation of the COR (d-C), respectively.

Table 1. Patient data summary

Patient	Affected side	Sex	Age at initial injury (years)	Age at examination (years)	Time from injury to examination (months)	Monteggia type	Ulnar deformity	Radial deformity	Initial treatment	ROM (pronation/supination) (°)	Chief complaint
1	Right	Male	5	14	108	1	6° ext, 4° valgus, 8° ER	None	Cast	90/90	Pain
2	Right	Male	5	8	38	1	9° ext, 21° IR	None	Cast	90/90	Pain
3	Right	Female	4	11	86	1	14° ext, 2° valgus, 5° ER	None	Pinning	90/90	Pain
4	Right	Male	7	38	372	1	3° ext, 1° valgus, 33° ER	None	Cast	90/90	PIN palsy
5	Right	Male	7	9	14	1	8° ext, 6° valgus, 13° ER	None	Pinning	60/70	Pain
6	Right	Female	6	14	96	1	11° ext, 6° valgus, 8° ER	None	Cast	90/90	Pain
7	Right	Male	5	32	324	1	4° ext, 2° varus, 8° ER	None	Cast	90/90	PIN palsy
8	Left	Female	7	9	24	4	3° ext, 5° valgus, 2° IR	9° ext, 2° valgus, 4° ER	Cast	90/80	Pain
9	Right	Male	12	14	21	4	14° ext, 9° varus, 1° IR	18° ext, 6° varus	Cast	90/90	Pain
10	Left	Male	12	13	6	4	3° ext, 11° valgus, 8° IR	30° ext, 2° varus, 20° IR	Cast	45/50	Pain
Average			7.0	16.2	109					83/83	

Ext = extension; ER = external rotation; IR = internal rotation; PIN = posterior interosseous nerve.

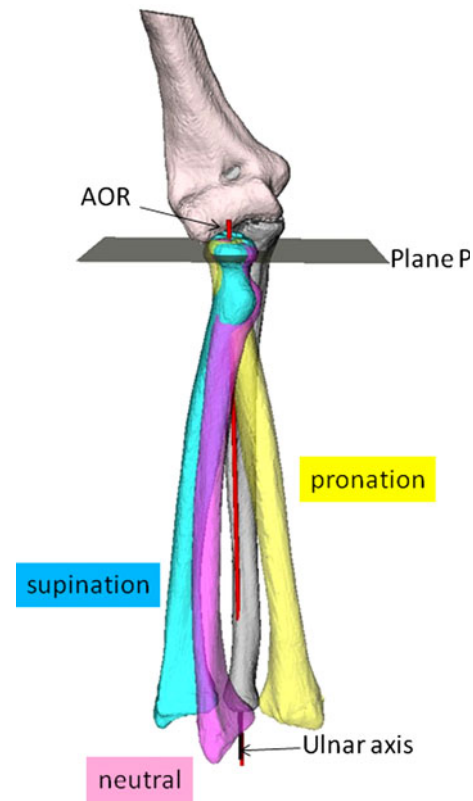


Fig. 1 A diagram illustrates the 3D bone models in three positions. The AOR (red) for the radius relative to the ulna was calculated. Plane P was defined as the plane perpendicular to the longitudinal axis of the ulna (black).

We determined six interosseous membrane ligament attachments (distal ligament of the accessory band, distal portion of the central band, middle portion of the central band, proximal portion of the central band, proximal oblique cord, and dorsal oblique accessory cord; Fig. 2) on the mirror image of the contralateral normal bones by combining osseous images and anatomic data of ligament attachments according to the method described by Moritomo et al. [22] and Noda et al. [25] (Fig. 2A). The attachments on the affected bones were determined by superimposing the mirror images of the bones with the ligament attachments onto the affected bones using a bone registration technique (Fig. 2B–C). Osseous deformity also could be determined in 3D using this technique [1, 23, 35]. The six paths were modeled on the affected side according to the method described by Marai et al. [19]; the method used to calculate the shortest ligaments takes into account that the ligament does not form a straight line from origin to insertion, but detours around bony protrusions (Fig. 2D). We then calculated the 3D distance of the six paths during forearm rotation [13, 21, 22]. The accuracy of this 3D volume registration technique for forearm bones using CT data was evaluated by Oka et al. [26]. The rotation error

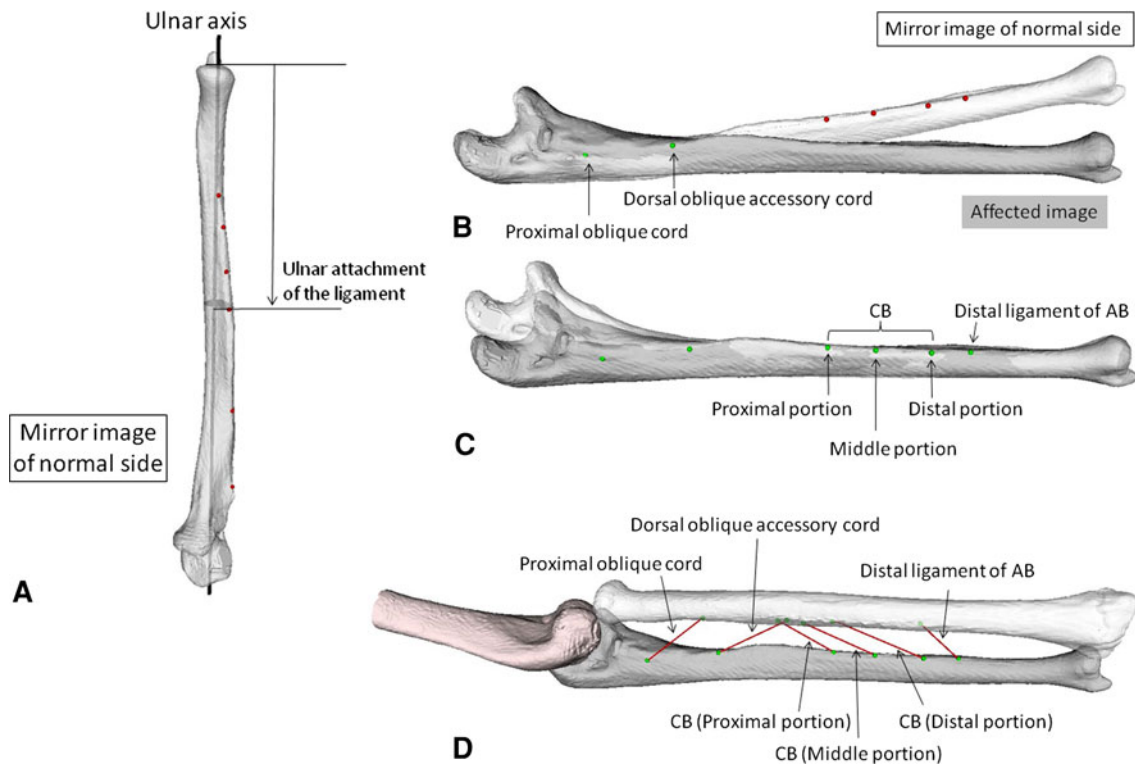


Fig. 2A–D (A) Determination of attachment sites of interosseous membrane ligaments on the contralateral bones is shown. Location of the center of attachment is expressed as a percentage of total bone length from the distal end of each bone. First, the 3D bone model was cut on a plane perpendicular to the longitudinal axis at the level of attachment according to the anatomic data. Then, an attachment point

was $0.38^\circ \pm 0.62^\circ$ and the translation error was 0.56 ± 0.06 mm.

All data were expressed as mean \pm SD. Because we speculated the kinematics of chronic radial head dislocation resulting from a Type 4 Monteggia lesion might be different from those of a Type 1 Monteggia lesion, differences in d-R, d-S, and d-C between these two groups were analyzed using the Mann–Whitney U test. In addition, previous researchers have reported the surgical outcome was less satisfactory for long-standing cases with a duration greater than 3 years from injury or older cases in patients older than 12 years [24, 34]. Therefore, differences in d-R, d-S, and d-C also were analyzed for the two groups based on factors (age at examination and time from injury to examination) that might influence kinematics. Paired t-tests were used to determine whether there were significant differences in interosseous membrane ligament length between forearm rotation positions [22]. To determine the influence of ulnar deformity on interosseous membrane ligament isometricity, correlations between the degrees of ulnar deformity and changes in interosseous membrane ligament length during forearm rotation in Type 1 lesions were examined using Pearson's correlation coefficient. A $p < 0.05$ was considered significant.

was placed on the interosseous border of the bone. Determination of attachment sites of interosseous membrane ligaments on the (B) proximal and (C) distal parts of the affected bones using a bone registration technique is shown. (D) A diagram illustrates the six interosseous membrane ligament models in chronic radial head dislocation. CB = central band; AB = accessory band.

Results

The radial head was relatively stable in the dislocated position during forearm rotation in Type 1 lesions (Fig. 3A), while it showed an unstable, clock motion pattern in Type 4 lesions (Fig. 3B). Age at examination and time from injury to examination had little influence on 3D kinematics (Table 2). d-R, d-S, and d-C were 2.4 ± 0.9 mm, 2.8 ± 2.0 mm, and 3.4 ± 2.4 mm, respectively, in Type 1 lesions, and 6.2 ± 1.0 mm, 10.2 ± 1.8 mm, and 4.7 ± 3.4 mm, respectively, in Type 4 lesions. The d-R and d-S were larger ($p = 0.02$ in both cases) in the Type 4 lesions than in the Type 1 lesions, whereas d-C was similar in the two groups ($p = 0.57$).

Three interosseous membrane ligaments showed little change in length in Type 1 lesions (Fig. 4), while no ligament showed an isometric pattern in Type 4 lesions (Fig. 5). The degree of ulnar deformity did not show a correlation with interosseous membrane ligament isometricity. In Type 1 lesions, the distal portion of the central band (Fig. 4A) and distal ligament of the accessory band (Fig. 4D) showed little change in length during supination but decreased during pronation ($p = 0.02$ and 0.003 , respectively), where the differences were 0.7 ± 0.5 mm

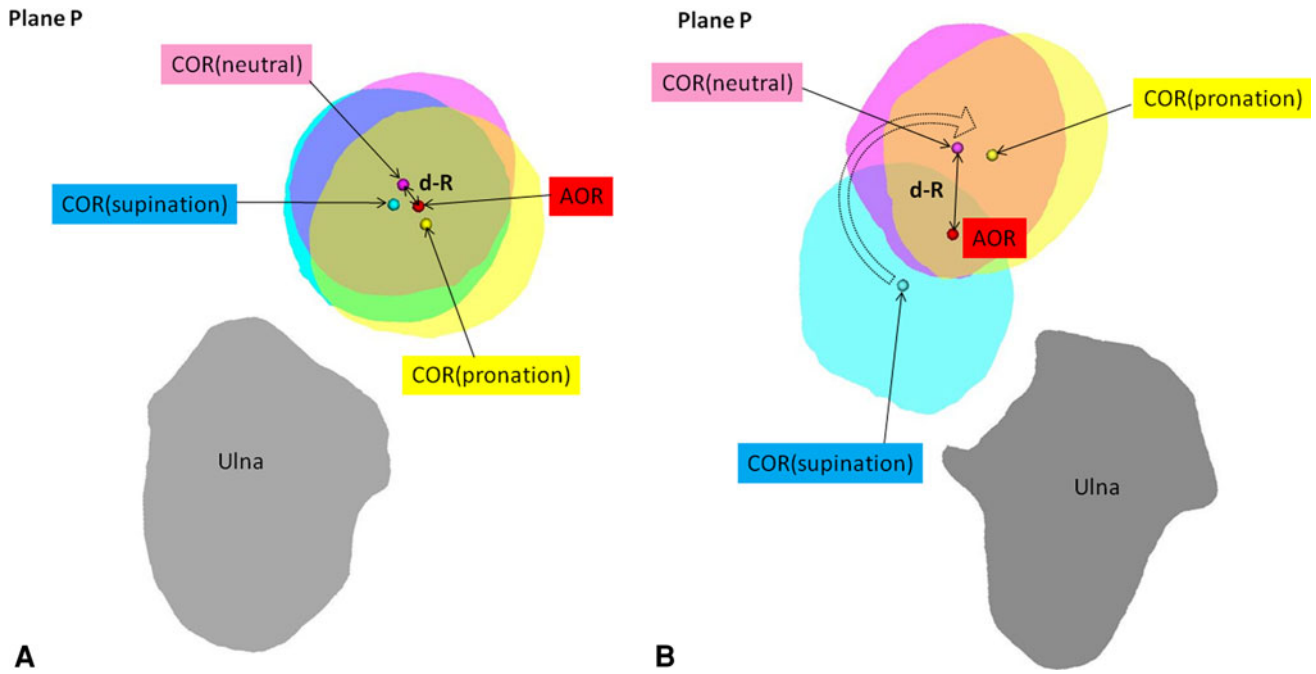


Fig. 3A–B The kinematics in (A) Type 1 and (B) Type 4 lesions are shown. In the Type 1 lesion, the radial head was relatively stable during forearm rotation, and d-R and COR translation were minimal, whereas in the Type 4 lesion, the radial head showed a pattern similar to clock motion during forearm rotation, and d-R and COR translation were large. COR = center of the radial head; d-R = distance from the COR to the mean axis of rotation (AOR).

Table 2. Factors influencing the three-dimensional kinematics

Factor	Number of patients	d-R (mm)	p value	d-S (mm)	p value	d-C (mm)	p value
Monteggia type							
Type 1	7	2.4 ± 0.9	0.02	2.8 ± 2.0	0.02	3.4 ± 2.4	0.57
Type 4	3	6.2 ± 1.0		10.2 ± 1.8		4.7 ± 3.4	
Age at examination							
≥ 12 years	6	3.4 ± 2.3	0.67	5.4 ± 4.0	0.92	4.0 ± 2.5	0.67
< 12 years	4	3.8 ± 1.8		4.5 ± 4.5		3.6 ± 3.2	
Time from injury to examination							
≥ 3 years	6	2.6 ± 1.0	0.13	2.7 ± 2.2	0.03	3.6 ± 2.5	1.00
< 3 years	4	5.1 ± 2.4		8.5 ± 3.7		4.1 ± 3.1	

Values are expressed as mean ± SD; d-R = distance from the center of the radial head to the mean axis of rotation; d-S = distance of sagittal translation of the center of the radial head; d-C = distance of coronal translation of the center of the radial head.

and 1.3 ± 0.7 mm, respectively. The middle (Fig. 4B) and proximal (Fig. 4C) portions of the central band and the proximal oblique cord (Fig. 4E) showed little change in length during rotation, showing a completely isometric pattern. Differences in length were within 1 mm (0.4 ± 0.3 mm, 0.5 ± 0.2 mm, and 0.5 ± 2.3 mm, respectively). The dorsal oblique accessory cord showed little change in length during pronation but decreased during supination (p = 0.02), where the difference was 1.3 ± 1.1 mm (Fig. 4F). The total angle of ulnar deformity was 24.6° ± 7.7° and did not show a correlation with changes in interosseous membrane ligament length (Table 3). In

Type 4 lesions, the distal (Fig. 5A), middle (Fig. 5B), and proximal (Fig. 5C) portions of the central band and the distal ligament of the accessory band (Fig. 5D) increased in length from supination to pronation, although these changes were not statistically significant. Differences in length were 1.4 ± 1.4 mm, 2.1 ± 2.0 mm, 1.6 ± 0.8 mm, and 6.5 ± 8.5 mm, respectively. The length of the proximal oblique cord increased during supination (p = 0.02), where the difference was 1.9 ± 0.5 mm (Fig. 5E). The length of the dorsal oblique accessory cord decreased during pronation (p = 0.009), where the difference was 4.2 ± 0.7 mm (Fig. 5F).

Fig. 4A–F The graphs show length change in six interosseous membrane ligaments in a Type 1 lesion: **(A)** distal, **(B)** middle, and **(C)** proximal portions of the central band; **(D)** distal ligament of the accessory band; **(E)** proximal oblique cord; and **(F)** dorsal oblique accessory cord. The middle portion of the central band, proximal portion of the central band, and proximal oblique cord showed little change in length. The length of the distal portion of the central band and distal ligament of the accessory band decreased under pronation and that of the dorsal oblique accessory cord decreased under supination.

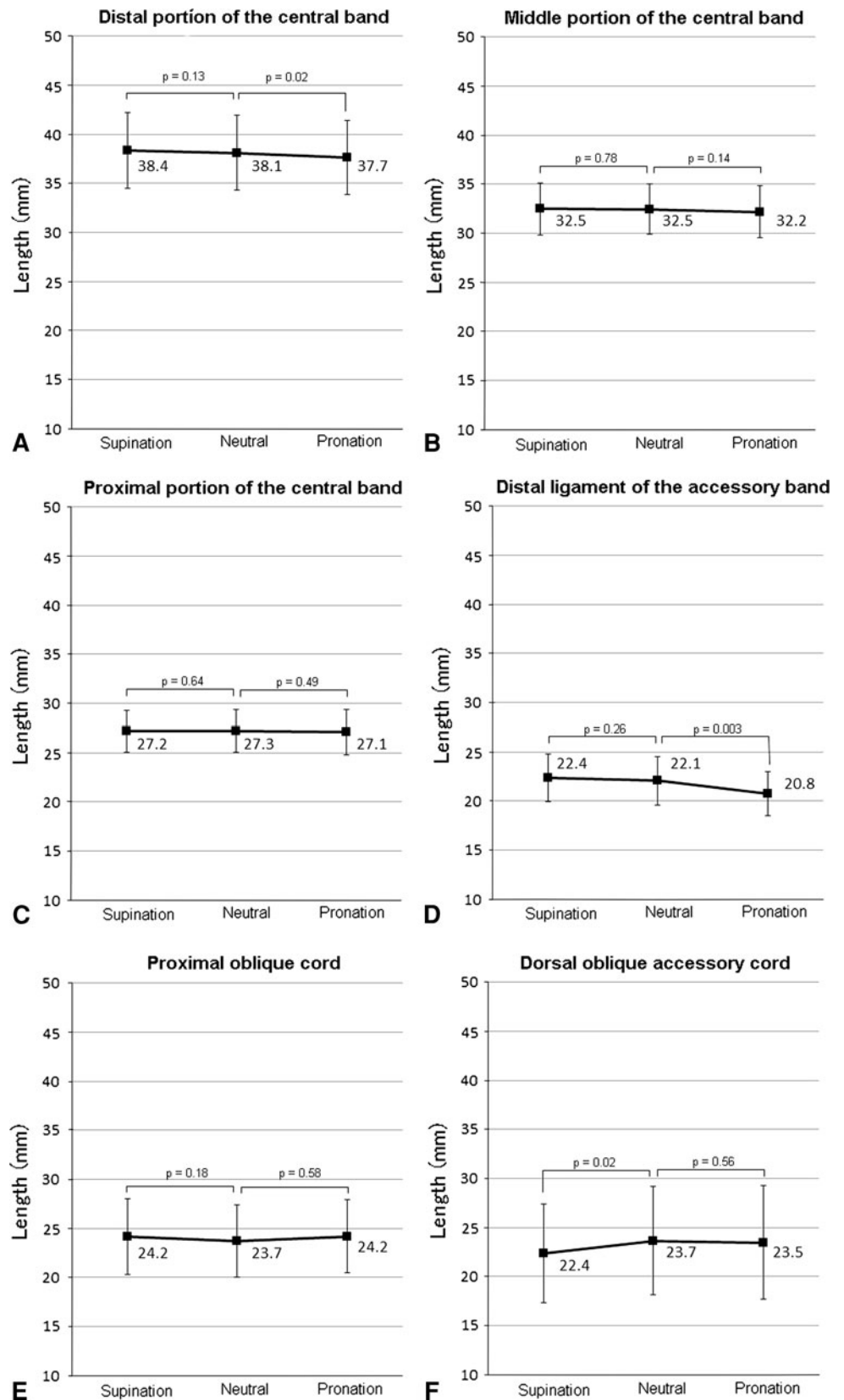


Fig. 5A–F The graphs show length change in six interosseous membrane ligaments in a Type 4 lesion: **(A)** distal, **(B)** middle, and **(C)** proximal portions of the central band; **(D)** distal ligament of the accessory band; **(E)** proximal oblique cord; and **(F)** dorsal oblique accessory cord. The length of the distal components (central band and accessory band) decreased under supination and that of the proximal components (proximal oblique cord and dorsal oblique accessory cord) decreased under pronation contrary to events in the normal forearm.

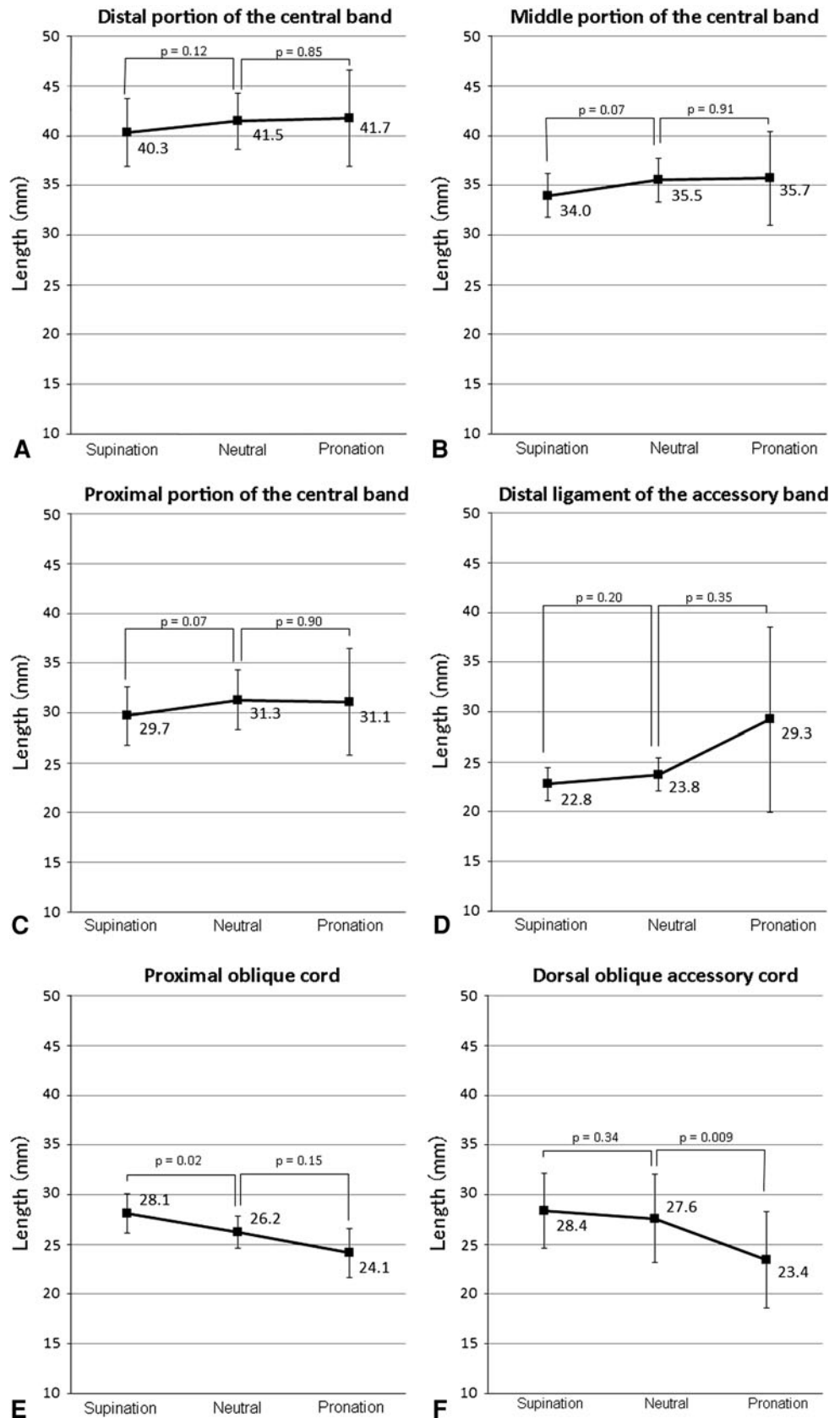


Table 3. Correlations between ulnar deformity and changes in interosseous membrane ligament length in patients with Type 1 dislocations

Interosseous membrane ligaments	p value
Distal portion of the central band	0.94
Middle portion of the central band	0.77
Proximal portion of the central band	0.32
Distal ligament of the accessory band	0.80
Proximal oblique cord	0.16
Dorsal oblique accessory cord	0.81

Discussion

Treatment for chronic radial head dislocations is controversial. Although the detailed kinematics and interosseous membrane function during forearm rotation in chronic radial head dislocation are unknown, several procedures have been performed to achieve reduction of the radial head. However, clinical results have not always been favorable. Researchers recently were able to measure joints *in vivo* and by 3D kinematics and thus calculate ligament length using noninvasive techniques [21, 22]. In this study, we investigated (1) the *in vivo* 3D kinematics and (2) the *in vivo* 3D length changes of the interosseous membrane ligaments during forearm rotation in chronic radial head dislocations using an advanced noninvasive technique.

Our study had some limitations. The number of patients, particularly with Type 4 Monteggia lesions ($n = 3$), was not large. Ligament attachments were determined only on the basis of anatomic information. Our findings are theoretical only and have not been tested surgically. The disadvantage of the analytic technique is the use of static motion analysis in only three positions. Static measurement does not include any inertial or functional effects that might occur during forearm rotation.

Regarding analysis of 3D kinematics, our results indicate the radial head was relatively stable during forearm rotation in Type 1 Monteggia lesions in comparison to the normal forearm [3, 14, 20, 36], although abnormal coronal translation of the radial head occurred by approximately 3 mm. However, the radial head was unstable during rotation in Type 4 Monteggia lesions. The AOR passed through a point approximately 6 mm from the COR, and abnormal translation of the radial head occurred approximately 10 mm in the sagittal direction and approximately 5 mm in the coronal direction. The differences in kinematics between the two groups may be attributable to the effect of radial deformity, which exists only in Type 4 lesions, and possible ligament laxity from the original injury.

In Type 1 lesions, the isometricity of the interosseous membrane ligaments was maintained in comparison to the normal forearm [22]. The middle and proximal portions of

the central band showed almost complete isometricity, and there was no laxity in pronation. In addition, the proximal oblique cord, which acts as a check line in the normal forearm, showed an isometric pattern during rotation. In the normal forearm, the length of the proximal oblique cord increases in pronation under the influence of the radial tuberosity [22, 30], but this was not noted in chronic radial head dislocation because of anterior shift of the radius. The isometricity of the interosseous membrane ligaments may contribute to relatively stable motion of the radial head in the dislocated position during rotation even when a functional annular ligament is absent. However, in Type 4 lesions, the normal pattern of the interosseous membrane ligaments during rotation was not recorded. In contrast to the normal pattern, the distal interosseous membrane ligaments were taut mainly in pronation, while the proximal interosseous membrane ligaments were taut mainly in supination.

Ulnar bending osteotomy, almost always with elongation, has been performed for treatment of chronic radial head dislocation [6, 7, 24, 34]. This surgery is expected to correct the position of the radial head based on the concept that the distal ulna and radius move together through the interosseous membrane, rather than to correct the ulnar bone deformity. The findings regarding change in length of the interosseous membrane ligaments in Type 1 lesions support this concept. Control of the radial head is considered to be reliable because the majority of the interosseous membrane ligaments were always taut in any forearm position. In addition, during rotation, the relative stability of the radial head is favorable to maintaining the position of the radial head in the proximal radioulnar joint after ulnar osteotomy. However, the radial head did not show totally normal kinematics. Additional ligament reconstruction may be necessary in patients with considerable coronal translation of the radial head. Conversely, an ulnar osteotomy may not control the radial head in Type 4 lesions because of its instability during rotation and the abnormal pattern of interosseous membrane ligament tautness. For Type 4 lesions, a radial osteotomy in addition to an ulnar osteotomy may be necessary to alter the path of the AOR to coincide with the COR. Nevertheless, the AOR and the distance between the radius and ulna (the interosseous membrane ligament length) may change after an ulnar osteotomy. Additional research, including computer simulation of the ulnar osteotomy regarding soft tissue effects or postoperative motion analysis is required to confirm the mechanism of an ulnar osteotomy.

We found the radial head was relatively stable during forearm rotation, and the isometricity of the interosseous membrane remained in Type 1 lesions. Conversely, the radial head was unstable during rotation, and the normal interosseous membrane ligament tautness pattern was disrupted in Type 4 lesions. We believe the information

derived from our study will improve our understanding of chronic radial head dislocations and contribute to appropriate surgical treatment. In addition, our analytic technique that includes the contralateral normal side is considered useful in addressing other difficult issues such as forearm diaphyseal malunion.

Acknowledgments We thank Hideki Yoshikawa MD, PhD; Shinsuke Omori MD; Yohei Kawanishi MD; Ryoji Nakao, computer programmer; Sumika Ikemoto, clinical assistant at the Department of Orthopedic Surgery, Osaka University Graduate School of Medicine; and Kunihiro Oka MD, PhD at the Department of Orthopedic Surgery, Bell-land General Hospital, for their contributions to this study.

References

- Athwal GS, Ellis RE, Small CF, Pichora DR. Computer-assisted distal radius osteotomy. *J Hand Surg Am.* 2003;28:951–958.
- Bado JL. The Monteggia lesion. *Clin Orthop Relat Res.* 1967;50:71–86.
- Baeyens JP, Van Glabbeek F, Goossens M, Gielen J, Van Roy P, Clarys JP. In vivo 3D arthrokinematics of the proximal and distal radioulnar joints during active pronation and supination. *Clin Biomech (Bristol, Avon).* 2006;21(suppl 1):S9–S12.
- Best TN. Management of old unreduced Monteggia fracture dislocations of the elbow in children. *J Pediatr Orthop.* 1994;14:193–199.
- Fowles JV, Sliman N, Kassab MT. The Monteggia lesion in children: fracture of the ulna and dislocation of the radial head. *J Bone Joint Surg Am.* 1983;65:1276–1282.
- Hirayama T, Takemitsu Y, Yagihara K, Mikita A. Operation for chronic dislocation of the radial head in children: reduction by osteotomy of the ulna. *J Bone Joint Surg Br.* 1987;69:639–642.
- Horii E, Nakamura R, Koh S, Inagaki H, Yajima H, Nakao E. Surgical treatment for chronic radial head dislocation. *J Bone Joint Surg Am.* 2002;84:1183–1188.
- Hotchkiss RN, An KN, Sowa DT, Basta S, Weiland AJ. An anatomic and mechanical study of the interosseous membrane of the forearm: pathomechanics of proximal migration of the radius. *J Hand Surg Am.* 1989;14:256–261.
- Hurst LC, Dubrow EN. Surgical treatment of symptomatic chronic radial head dislocation: a neglected Monteggia fracture. *J Pediatr Orthop.* 1983;3:227–230.
- Inoue G, Shionoya K. Corrective ulnar osteotomy for malunited anterior Monteggia lesions in children: 12 patients followed for 1–12 years. *Acta Orthop Scand.* 1998;69:73–76.
- Kadic MA, Bloem RM. Traumatic isolated anterior dislocation of the radial head: a case with a 32-year follow-up. *Acta Orthop Scand.* 1991;62:288–289.
- Kalamchi A. Monteggia fracture-dislocation in children: late treatment in two cases. *J Bone Joint Surg Am.* 1986;68:615–619.
- Kataoka T, Moritomo H, Miyake J, Murase T, Yoshikawa H, Sugamoto K. Changes in shape and length of the collateral and accessory collateral ligaments of the metacarpophalangeal joint during flexion. *J Bone Joint Surg Am.* 2011;93:1318–1325.
- Kim HJ, Yi JH, Jung JW, Cho DW, van Riet R, Jeon IH. Influence of forearm rotation on proximal radioulnar joint congruency and translational motion using computed tomography and computer-aided design technologies. *J Hand Surg Am.* 2011;36:811–815.
- Kinzel GL, Hall AS Jr, Hillberry BM. Measurement of the total motion between two body segments. I: Analytical development. *J Biomech.* 1972;5:93–105.
- Kinzel GL, Hillberry BM, Hall AS Jr, Van Sickle DC, Harvey WM. Measurement of the total motion between two body segments. II: Description of application. *J Biomech.* 1972;5:283–293.
- Lichter RL, Jacobsen T. Tardy palsy of the posterior interosseous nerve with a Monteggia fracture. *J Bone Joint Surg Am.* 1975;57:124–125.
- Lloyd-Roberts GC, Bucknill TM. Anterior dislocation of the radial head in children: aetiology, natural history and management. *J Bone Joint Surg Br.* 1977;59:402–407.
- Marai GE, Laidlaw DH, Demiralp C, Andrews S, Grimm CM, Crisco JJ. Estimating joint contact areas and ligament lengths from bone kinematics and surfaces. *IEEE Trans Biomed Eng.* 2004;51:790–799.
- Matsuki KO, Matsuki K, Mu S, Sasho T, Nakagawa K, Ochiai N, Takahashi K, Banks SA. In vivo 3D kinematics of normal forearms: analysis of dynamic forearm rotation. *Clin Biomech (Bristol, Avon).* 2010;25:979–983.
- Moritomo H, Murase T, Arimitsu S, Oka K, Yoshikawa H, Sugamoto K. The in vivo isometric point of the lateral ligament of the elbow. *J Bone Joint Surg Am.* 2007;89:2011–2017.
- Moritomo H, Noda K, Goto A, Murase T, Yoshikawa H, Sugamoto K. Interosseous membrane of the forearm: length change of ligaments during forearm rotation. *J Hand Surg Am.* 2009;34:685–691.
- Murase T, Oka K, Moritomo H, Goto A, Yoshikawa H, Sugamoto K. Three-dimensional corrective osteotomy of malunited fractures of the upper extremity with use of a computer simulation system. *J Bone Joint Surg Am.* 2008;90:2375–2389.
- Nakamura K, Hirachi K, Uchiyama S, Takahara M, Minami A, Imaeda T, Kato H. Long-term clinical and radiographic outcomes after open reduction for missed Monteggia fracture-dislocations in children. *J Bone Joint Surg Am.* 2009;91:1394–1404.
- Noda K, Goto A, Murase T, Sugamoto K, Yoshikawa H, Moritomo H. Interosseous membrane of the forearm: an anatomical study of ligament attachment locations. *J Hand Surg Am.* 2009;34:415–422.
- Oka K, Doi K, Suzuki K, Murase T, Goto A, Yoshikawa H, Sugamoto K, Moritomo H. In vivo three-dimensional motion analysis of the forearm with radioulnar synostosis treated by the Kanaya procedure. *J Orthop Res.* 2006;24:1028–1035.
- Oka K, Murase T, Moritomo H, Goto A, Sugamoto K, Yoshikawa H. Accuracy analysis of three-dimensional bone surface models of the forearm constructed from multidetector computed tomography data. *Int J Med Robot.* 2009;5:452–457.
- Oka K, Murase T, Moritomo H, Sugamoto K, Yoshikawa H. Morphologic evaluation of chronic radial head dislocation: three-dimensional and quantitative analyses. *Clin Orthop Relat Res.* 2010;468:2410–2418.
- Oner FC, Diepstraten AF. Treatment of chronic post-traumatic dislocation of the radial head in children. *J Bone Joint Surg Br.* 1993;75:577–581.
- Patel BA. Form and function of the oblique cord (chorda obliqua) in anthropoid primates. *Primates.* 2005;46:47–57.
- Rodgers WB, Waters PM, Hall JE. Chronic Monteggia lesions in children: complications and results of reconstruction. *J Bone Joint Surg Am.* 1996;78:1322–1329.
- Seel MJ, Peterson HA. Management of chronic posttraumatic radial head dislocation in children. *J Pediatr Orthop.* 1999;19:306–312.
- Skahen JR 3rd, Palmer AK, Werner FW, Fortino MD. The interosseous membrane of the forearm: anatomy and function. *J Hand Surg Am.* 1997;22:981–985.
- Stoll TM, Willis RB, Paterson DC. Treatment of the missed Monteggia fracture in the child. *J Bone Joint Surg Br.* 1992;74:436–440.

35. Takeyasu Y, Murase T, Miyake J, Oka K, Arimitsu S, Moritomo H, Sugamoto K, Yoshikawa H. Three-dimensional analysis of cubitus varus deformity after supracondylar fractures of the humerus. *J Shoulder Elbow Surg.* 2011;20:440–448.
36. Tay SC, van Riet R, Kazunari T, Amrami KK, An KN, Berger RA. In-vivo kinematic analysis of forearm rotation using helical axis analysis. *Clin Biomech (Bristol, Avon).* 2010;25:655–659.
37. Wang MN, Chang WN. Chronic posttraumatic anterior dislocation of the radial head in children: thirteen cases treated by open reduction, ulnar osteotomy, and annular ligament reconstruction through a Boyd incision. *J Orthop Trauma.* 2006;20:1–5.